

# Mesoporous Silicon / Polypyrrole Based Structures for Paranitrophenol Sensing

fatma zohra tighilt (✉ [mli\\_zola@yahoo.fr](mailto:mli_zola@yahoo.fr))

CRTSE <https://orcid.org/0000-0002-1750-4163>

Samia BELHOUSSE

CRTSE

Anis Rahal

ENP: Ecole Nationale Polytechnique

KHALED Hamdani

CRTSE

Naima Belhaneche

ENP

Sabrina Sam

CRTSE

Kahina Lasmi

CRTSE

---

## Research Article

**Keywords:** Conducting polymers, Mesoporous silicon, Surface modification, Sensors

**Posted Date:** February 23rd, 2021

**DOI:** <https://doi.org/10.21203/rs.3.rs-224123/v1>

**License:**  This work is licensed under a Creative Commons Attribution 4.0 International License.

[Read Full License](#)

---

# Abstract

Elaboration of new structures based on semi-conductors and conducting polymers can procure a new alternative to the development of various electrochemical sensors with good sensibility.

The key idea of this paper is to develop a facile technique for the detection of the para-nitrophenol which is considered as an important toxic pollutant. In this context, different structures based on mesoporous silicon modified with Polypyrrole (PPy) were elaborated.

The hybrid structures have been characterized by several techniques such as FTIR, SEM and Contact angle measurements.

In addition, the behavior of these new structures for para-nitrophenol detection by cyclic voltammetry was studied. The results show a high sensitivity of the sensor in a large concentration interval.

## Introduction

Paranitrophenol (P-Nph) is a phenolic compound having a nitro-group opposed to the hydroxyl group on the benzyl ring. It is used in various industries and it is considered as an important toxic pollutant resulting from the biodegradation of pesticides [1].

Pesticides are chemical substances used to kill unwanted organisms and are a vital input in today's agriculture, protecting food from diseases. Unfortunately, pesticides often act as poisons for animals, humans and environment [2]. Therefore, the detection of these organic pollutants has become extremely important in recent years.

Hybrid structures are playing a very important role in the development of organic sensors by assembling two materials: organic and inorganic. The combination of these two phases has enabled to obtain materials with new properties and offering many advantages in different applications and takes a significant place in nanotechnology projects.

Sensors based on semiconductors and conducting polymers have significant potential and are taking a growing place in the development of public health and environment control. These sensors have rapid detection, high sensitivity, small size, and specificity in atmospheric conditions [3]. Particularly, polypyrrole (PPy) has received a special attention because of its physicochemical properties, high electrical conductivity and good stability [4]. PPy has been used in corrosion protection [5], drug delivery [6, 7], sensors [8, 9] and actuators [10, 11].

Besides, due to its excellent proprieties, mesoporous silicon has been considered as an important semiconductor material with a large range of applications [12].

In this work, a simple approach was utilized to fabricate an electrochemical sensor based on polypyrrole modified mesoporous silicon and oxidized mesoporous silicon to the electrochemical detection of para-

nitrophenol.

## Experiment

### Porous silicon preparation

Silicon samples were cut from double side polished (100)-oriented boron-doped p-type silicon wafers (0.06-0.08  $\Omega\text{cm}$  resistivity). They were cleaned with trichloroethylene, acetone and ethanol for few minutes. Then, they were rinsed with Milli-Q water. The native oxide was removed by immersing the samples in 10% aqueous HF for 1 min.

The mesoporous silicon (PSi) was obtained by electrochemical anodization in fluorhydric acid solution HF/deionized water/ ethanol (2/2/1). A constant current density of  $80 \text{ mA cm}^{-2}$  was applied for 30 s, as described elsewhere [13]. After etching, the samples were rinsed with pure ethanol and dried under a dry nitrogen stream prior to use.

### Oxidation of PSi surface

The hydrogen-terminated PSi surfaces were oxidized in an oven at  $200^\circ\text{C}$  for 24 h.

### Electrochemical polymerization study

Pyrrole was used without further purification and was stored at  $5^\circ\text{C}$  in the refrigerator. Polymerization was performed electrochemically in three compartment cell using a potentiostat (Model VMP3). PSi or oxidized PSi was used as working electrode. The counter electrode was a gold wire. All potentials were referred to saturated calomel electrode (SCE). Electropolymerization was carried out at ambient temperature ( $25 \pm 2^\circ\text{C}$ ). Modification of the porous silicon by polypyrrole could increase the surface sensitivity to the pollutant.

PPy deposition was performed by electrochemical oxidation of 0.01M pyrrole ( $\text{C}_4\text{H}_5\text{N}$ ) monomer in acetonitrile ( $\text{CH}_3\text{CN}$ ) solution with 0.1%  $\text{H}_2\text{O}$  containing 0.1M tetrabutylammonium tetrafluoroborate ( $\text{C}_{16}\text{H}_{36}\text{BF}_4\text{N}$ ) as supporting electrolyte. During the many assays performed for PPy electrodeposition, it has been noticed that the addition of different amounts of water in the grafting solution leads to the variation of the intensity and the form of the oxidation peak obtained during the electrochemical reaction. In the same way, Zhou and al. [14] confirmed that the electropolymerization of pyrrole was optimal when the proportion of water was in the order of 1% of the volume (acetonitrile / water), this is explained by the fact that water becomes a base more Strong as the pyrrole and can compete by effectively removing the protons released during the reaction and prevents further protonations of pyrrole.

The films deposited on PSi and on oxidized PSi were rinsed thoroughly with acetonitrile in order to eliminate PPy film excess which is no adsorbed at the surface.

The structures PSi /PPy and PSi oxide/PPy were characterized by FTIR, SEM and contact angle.

## Results And Discussion

The formation of mesoporous silicon is confirmed by surface SEM observations in our previous work [15], showing homogeneously distributed pores over the entire sample surface. The average pore size is in the range of 10-15 nm. The same morphologies were observed after thermal oxidized of porous silicon sample to stabilize its surface. We note that the mesopores are still discernible

FTIR spectroscopy has been proved to be a very powerful technique to detect the intermolecular interaction between the polymer and the interface. Figure (1) shows the infrared spectrum of porous silicon before and after oxidation. Before the oxidation, the mesoporous silicon exhibits three bands due to  $\nu\text{Si-Hx}$  stretching modes ( $x=1,2,3$ ) localized at 2090, 2110 and 2150  $\text{cm}^{-1}$ , a band at 910  $\text{cm}^{-1}$  ascribed to  $\delta\text{Si-H}_2$  scissor mode and two bands at 630 and 680  $\text{cm}^{-1}$  corresponding to  $\delta\text{SiHx}$ . The homogeneity of the porous layer is confirmed by the presence of periodic oscillations (figure (1)) [16].

After the surface oxidation, the infrared spectra confirm the significant oxidation of the PSi surface as it is indicated by the decrease of  $\nu\text{Si-Hx}$  and  $\delta\text{SiHx}$  bands [17]. An important vibration band of the Si-O bond containing the symmetric and antisymmetric mode stretching vibration of the Si-O-Si bond at 1107 $\text{cm}^{-1}$  and 1163  $\text{cm}^{-1}$ , respectively[18], and the SiO<sub>2</sub> stretching vibration at 1147  $\text{cm}^{-1}$ . We note again the appearance of a broad absorption between 3480 and 2900  $\text{cm}^{-1}$  due to terminal hydroxyl groups (Si OH) and likely to adsorbed water molecules.

Contact angle measurements provide an indication of the surface reactions efficiency. The contact angle of the mesoporous silicon determined by this method is 122° indicating the hydrophobic behavior of this surface (Figure (2.a)). After the oxidation of PSi surface, we observe a decrease in contact angle to 13° (Figure (2b)).

### Functionalization of PSi surface by PPy

Figure (3) shows the cyclic voltammogram of 0.01M pyrrole in anhydrous acetonitrile solution containing 0.1 M  $\text{C}_{16}\text{H}_{36}\text{BF}_4$ , on mesoporous silicon electrode, between -2 V and 3 V with a scan rate of 50  $\text{mV s}^{-1}$ . Pyrrole oxidation has two irreversible features; we observe the appearance of a shoulder located at approximately 1.14 V and a peak at 2 V corresponding to the formation of a radical cation and a dication during pyrrole monomer oxidation. The formation of PPy was visually observed. Since the number of electropolymerization cycles determines the thickness of polypyrrole layer, we preferred to stop the scanning after two cycles to prevent the polymer detachment. Indeed, in previous manipulations we found that PPy layer is not stable on the porous silicon beyond three scans.

The surface of PSi/PPy structure is characterized by SEM. The side view shows the PPy film forming a thick layer (Figure (4)). However, the PPy film does not adhere to the surface substrate suggesting that the structure obtained is a deposit and not a covalent grafting.

Researchers have faced the same problem of adherence when studying polypyrrole deposition on various substrates and several methods have been proposed to overcome this problem [19]. In this work, we have proceeded to a thermal oxidation of the PSi hydride surface to compensate for the low adherence of the polymer.

### **Functionalization of oxidized PSi surface by PPy**

Figure (5) shows the cyclic voltammogram of 0.01M pyrrole in anhydrous acetonitrile solution containing 0.1 M  $C_{16}H_{36}BF_4$ , on oxidized mesoporous silicon electrode, between -2 V and 2V. Scan rate = 50 mV s<sup>-1</sup>. We observed in the first scan a shoulder at 0.5 V, corresponding to the monomer oxidation to form cation radical leading to the formation of the polypyrrole layer.

In the reverse scan, we observed a cathodic peak located at 0.1 V characteristic of the reduction of the polymer deposit formed during the polymerization reaction. During the recording of further cyclovoltammograms as depicted in Figure (5), the oxidation peak current shifts to positive values and the reduction peak shifts to negative values. The displacement of these potentials is accompanied by an increase of the current intensity of the oxidation and reduction peaks confirming the deposition of the polypyrrole film on the oxide mesoporous silicon surface. With repeated cycles, an increasingly thick dark film was deposited on the oxidized porous silicon surface.

Figure (6) shows SEM micrographs of PPy films deposited with cyclic voltammetry (CV) on oxidized mesoporous silicon surface. The obtained film is thin and appears homogeneous over the whole surface. The deposit is characterized by a cauliflower-like structure consisting of microspherical grains of approximately 1µm diameter. A. El Jouahri and al obtain the same morphologies on the study of the electrochemical behavior of PPy coated carbon steel in aqueous NaCl solution by scanning electrochemical microscopy [20-21].

This modification was confirmed by another technique. The FTIR spectra depicted in the figure (7) in the range 450–4000 cm<sup>-1</sup> show the presence of the major expected peaks of the PPy on the oxidized PSi surface.

The absorption centered at 1541 cm<sup>-1</sup> and 1462 cm<sup>-1</sup> correspond to the c-c and c-n vibration pyrrole rings. Also the peaks at 1298, 1180 and 1039 cm<sup>-1</sup> can be attributed to the C-H plane stretch vibration. The peak at 963 ascribed to the C-C out of plane deformation [22].

### **Electrochemical Behavior of 4-NP:**

The electrochemical behavior of 4-NP at the PSi/PPy hybrid structure was investigated using cyclic voltammetry (CV).

After addition of para-nitrophenol, the voltammetric behavior as shown in Figure (8) is strongly affected and the shape of the curve is modified. The different structures were tested in a concentration range of

$10^{-2}$  to  $10^{-8}$ M. A large peak appears around 1.7 V. We note a shift of this peak with the variation of the concentration. The oxidation peak may be attributed to the oxidation of the 4-(hydroxyamino)phenol which is the reduction reaction product of the paranitrophenol [23].

### **Calibration graph:**

The calibration curve for p-NPh in tampon PBS solution was investigated in terms of the relationship between p-NPh concentration and the current oxidation peak.

The calibration curve (Figure (9)) shows that the intensity of oxidation peaks increases linearly with the concentration of p-Nph. The linearity is obtained over a concentration range of  $10^{-2}$  to  $10^{-8}$ M with regression coefficients of 0.959, which implies a good calibration of this detector and it can be used in a large concentration range. We can conclude from these results that the hybrid systems PSi Oxide/PPy are sensitive to para-nitrophenol.

## **Conclusions**

The deposition of polypyrrole on oxidized porous silicon substrate using electrochemical methods was successfully achieved. The linearity is obtained over a concentration range of  $10^{-2}$  to  $10^{-8}$ M, which implies a good calibration of this detector and it can be used in a large concentration range. These results have shown that the hybrid structures PSi Oxide / PPy are sensitive to para-nitrophenol.

## **Declarations**

### **Acknowledgments**

The authors would like to thank the General Directorate for Scientific Research (DGRSDT) and the Semiconductor Research Center for Energy (CRTSE) for their financial support.

**Funding:** All of the sources of funding for the work described in this publication are financed by the General Directorate for Scientific Research (DGRSDT) and the Semiconductor Research Center for Energy (CRTSE).

**Conflicts of interest/Competing interests:** We wish to confirm that there are no known conflicts of interest associated with this publication.

**Availability of data and material:** The datasets generated during and/or analyzed during the current study are available from the corresponding author on reasonable request.

**Code availability:** we did not use codes.

**Author's contributions:**

**Tighilt:** Initiation of the work, polypyrrole grafting on the mesoporous silicon and interpretation of the results.

**Belhousse:** Interpretation of FT-IR results.

**Rahal:** Accomplishment of para-nitrophenol electro-detection.

**Belhaneche:** Contribution to the correction of the article.

**Hamdani:** Interpretation of MEB results.

**Lasmi:** Characterization of different structures by contact angle measurements.

**Sam:** Elaboration and characterization of mesoporous silicon.

**Ethics approval:** 'Not applicable' for that section.

**Consent to participate:** 'Not applicable' for that section.

**Consent for publication:** 'Not applicable' for that section.

## References

1. Y. Cheng, Y. Li, D. Li, B. Zhang, R. Hao, and S.Sang (2017) A sensor for detection of 4-nitrophenol based on a glassy carbon electrode. Modified with a reduced grapheme oxide / Fe<sub>3</sub>O<sub>4</sub> nanoparticle composite. *International Journal of Electrochemical Science* 127754 – 7764.
2. Gamal A. E. Mostafa (2010) Electrochemical Biosensors for the Detection of Pesticides, the *Open Electrochemistry Journal* 2: 22-24.
3. B. Lakard, S. Carquigny, O. Segut , T. Patois and S. Lakard (2015) Gas Sensors Based on Electrodeposited Polymers. *Metals*, 5:1371-1386.
4. A.B.Moghaddam, T.Nazari, J.Badraghi, M.Kazemzad (2009) Synthesis of ZnO Nanoparticles and Electrodeposition of Polypyrrole/ZnO Nanocomposite Film, *Int. J. Electrochem. Sci.*, 4247 – 257.
5. T. Ohtsuka (2012) Corrosion Protection of Steels by Conducting Polymer Coating, *international journal of corrosion*, Article ID 915090, 1-7.
6. S. Geetha, C. R.K. Rao, M. Vijayan, D.C. Trivedi (2006) Biosensing and drug delivery by polypyrrole, *Analytica Chimica Acta* 568: 119–125.
7. S.S.A. Ali, M. Firlak, S. R. Berraw, N. R. Halcovitch, S. J. Baldock, B. M. Yousafzai, R. M. Hathout, J. G. Hardy (2018) Electrochemically Enhanced Drug Delivery Using Polypyrrole Films, *Materials*, 11(7) 1123.
8. M.A.Chaugule, S.G. Pawar, S.L. Patil, B.T. Raut, P. Godse, S. Sen, V. Patil (2011) Polypyrrole Thin Film: Room Temperature Ammonia Gas Sensor, *IEEE Sensors Journal*, 11(9): 2137-2141.

9. M. A. Tuana, D. T. Phama, T. X. Chua, N. M. Hieub, N. H. Hai (2014) Highly sensitive DNA sensor based on polypyrrole nanowire, *Applied Surface Science*, 309:285–289.
10. B. Yan, Y. Wu and L. Guo (2017) Recent Advances on Polypyrrole Electroactuators, *Polymers*, 9, 446:1-20.
11. S. Demoustier-Champagne, E. Ferain, C. Jerome, R. Gerome, R. Legras (1998) Electrochemically synthesized polypyrrole nanotubules: effects of different experimental conditions, *European Polymer Journal*, 34,12:1767-1774.
12. D.C. Tessier, S. Boughaba, M. Arbour, P. Roos, G. Pan (2006) Improved surface sensing of DNA on gas-etched porous silicon, *Sensors and Actuators B* 120: 220–230.
13. S. Sam, L. Touahir, J. Salvador Andresa, P. Allongue, J.N. Chazalviel, A.C. Gouget Laemmel, C. Henry de Villeneuve, A. Moraillon, F. Ozanam, N. Gabouze, S. Djebbar (2010) semi-quantitative study of the EDC/NHS , activation of acid terminal groups at modified porous silicon surfaces *Langmuir*, 19;26(2):809-14.
14. M. Zhou, J. Heinze (1999) Electropolymerization of pyrrole and electrochemical study of polypyrrole: Evidence for structural diversity of polypyrrole. *Electrochimica Acta*, 44 (11):1733-1748.
15. K. Khaldi, S. Sam, A. Lounas, C. Yaddaden, N.E. Gabouze (2017) Comparative investigation of two methods for Acetylcholinesterase enzyme immobilization on modified porous silicon, *Applied Surface Science*, 421: 148-154.
16. K. Lasmi, H. Derder, A. Kermad, S. Sam, H. Boukhalifa-Abib, Samia Belhousse a, F. Z. Tighilt, K. Hamdani, N. Gabouze (2018) Tyrosinase immobilization on functionalized porous silicon surface for optical monitoring of pyrocatechol, *Applied Surface Science*, 446:3-9.
17. F.Z. Tighilt, F. Zane, N. Belhaneche-Bensemra, S. Belhousse, S. Sam, N. Gabouze (2013) Electrochemical gas sensors based on polypyrrole-porous silicon, *Applied Surface Science* 269: 180–183.
18. S. Belhousse, R. Boukherroub, S. Szunerits, N. Gabouze, A. Keffous, S. Sam, A. Benaboura (2010) Electrochemical grafting of poly(3-hexylthiophene) on porous silicon for gas sensing, *Surface and Interface Analysis*, 42 (6-7):1041–1045.
19. F. Beck, R. Michaelis (1992) Strongly adherent smooth coatings of polypyrrole oxalate on iron, *Journal Coatings Technology*, 6459–67.
20. A. El Jaouhari, D. Filota, A. Kiss, M. Laabd, E. A. Bazzaoui, L. Nagy, G. Nagy, A. Albourine, J. I. Martins, R. Wang, M. Bazzaoui (2016) SECM investigation of electrochemically synthesized polypyrrole from aqueous medium, *Journal of Applied Electrochemistry* 46 (12):1199-1209.
21. A. El Jaouharia , M. Laabda , E.A. Bazzaouib , A. Albourinea , J.I. Martinsc , R. Wangd , G. Nagye , M. Bazzaoui (2015) Electrochemical and spectroscopical studies of polypyrrole synthesized on carbon steel from aqueous medium, *Synthetic Metals*, 209:11–18.
22. R. Kanthapazham, C. Ayyavu and D. Mahendiradas (2016) Removal of Pb<sup>2+</sup>, Ni<sup>2+</sup> and Cd<sup>2+</sup> ions in aqueous media using functionalized MWCNT wrapped polypyrrole nanocomposite, *Desalination and Water Treatment*, 57,136:16871-16885.

23. G. B.P. Ngassa, I. Tonlé, E. Ngameni (2016) Square wave voltammetric detection by direct electroreduction of paranitrophenol (PNP) using anorganosmectite film-modified glassy carbon electrode, Talanta, 147:547-555.

## Figures

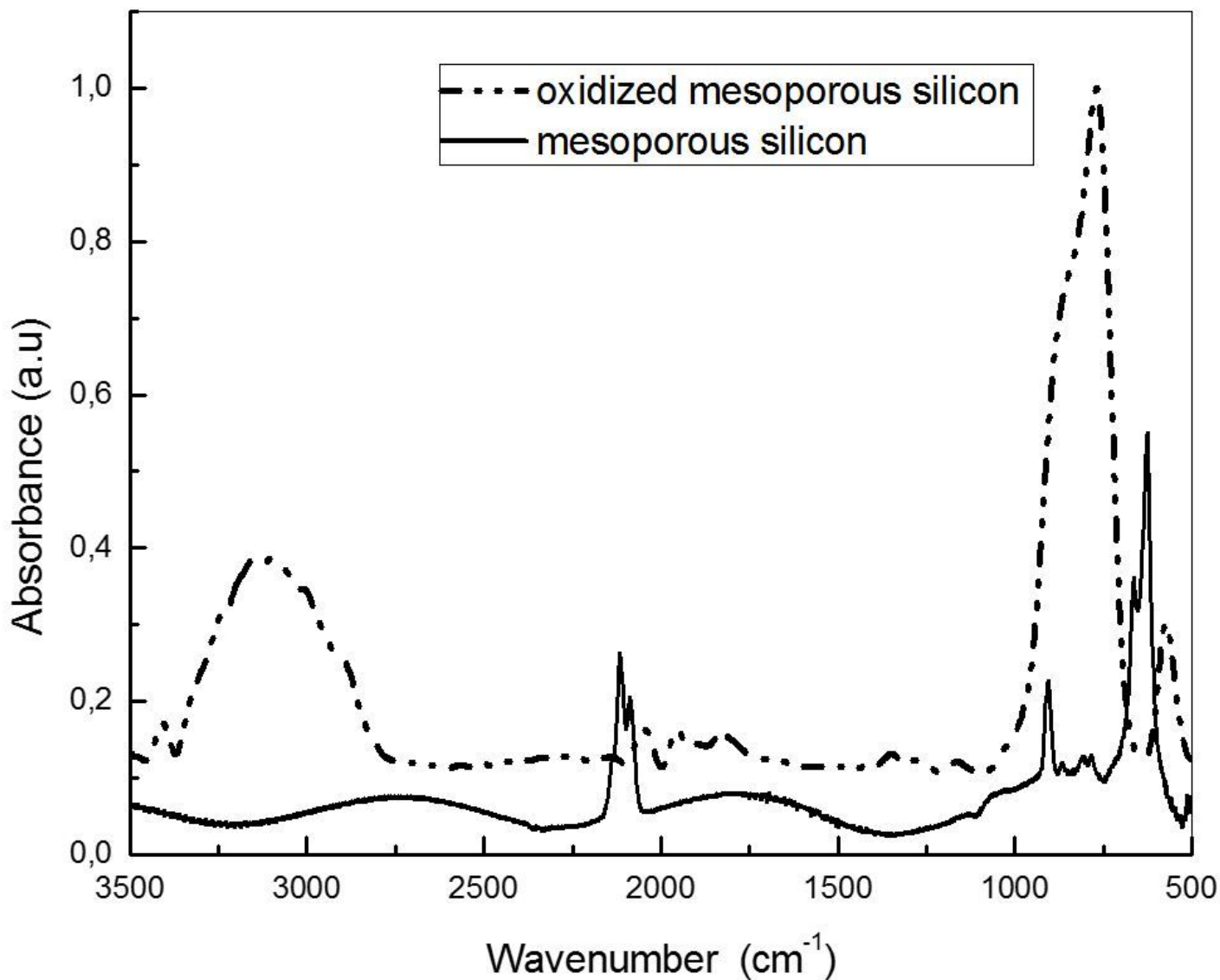
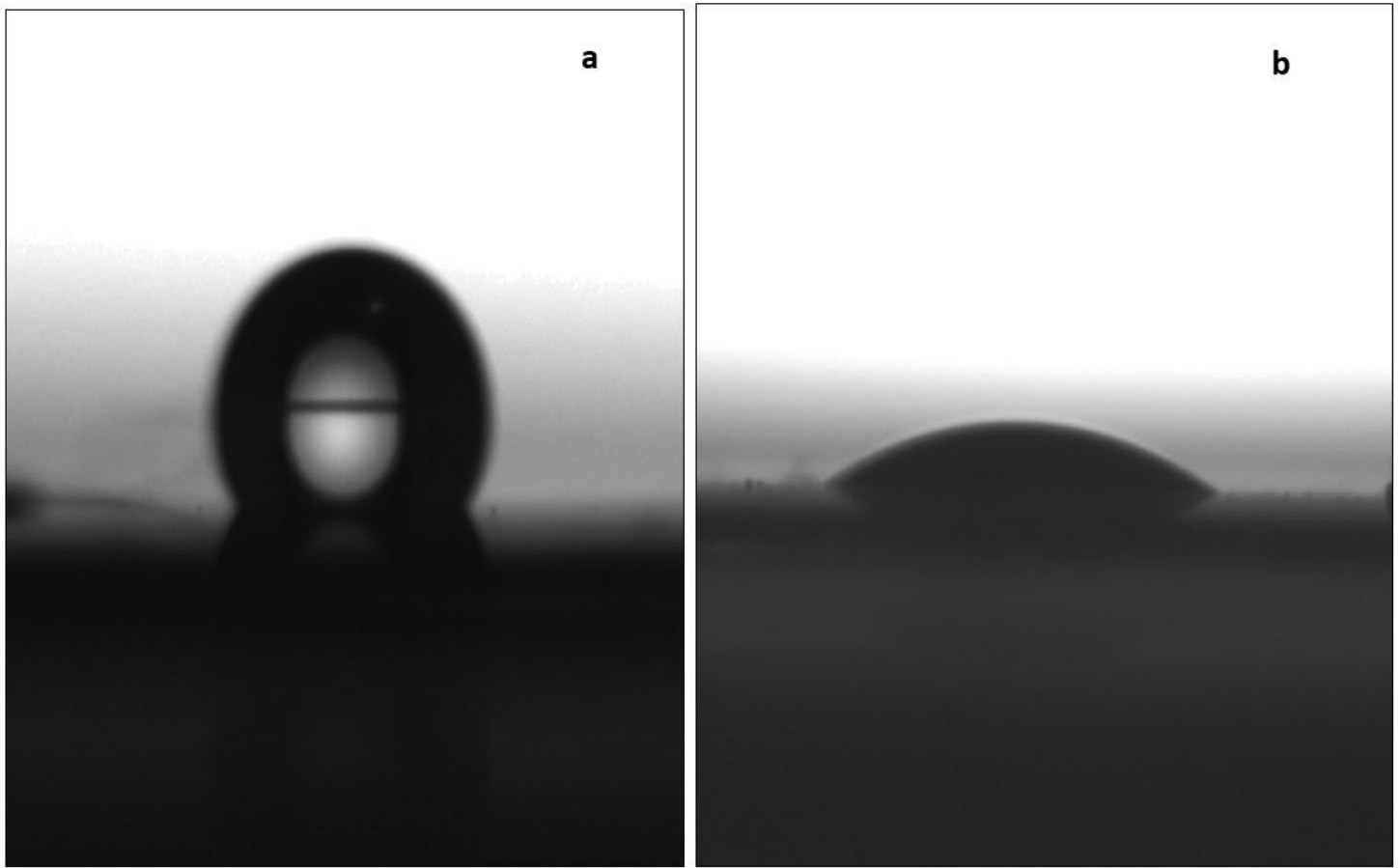


Figure 1

FTIR spectra of PSi and oxidized PSi .



**Figure 2**

Contact angle of a 1  $\mu$ l of water drop on PSi surface: (a) after PSi formation, (b) after PSi oxidation.

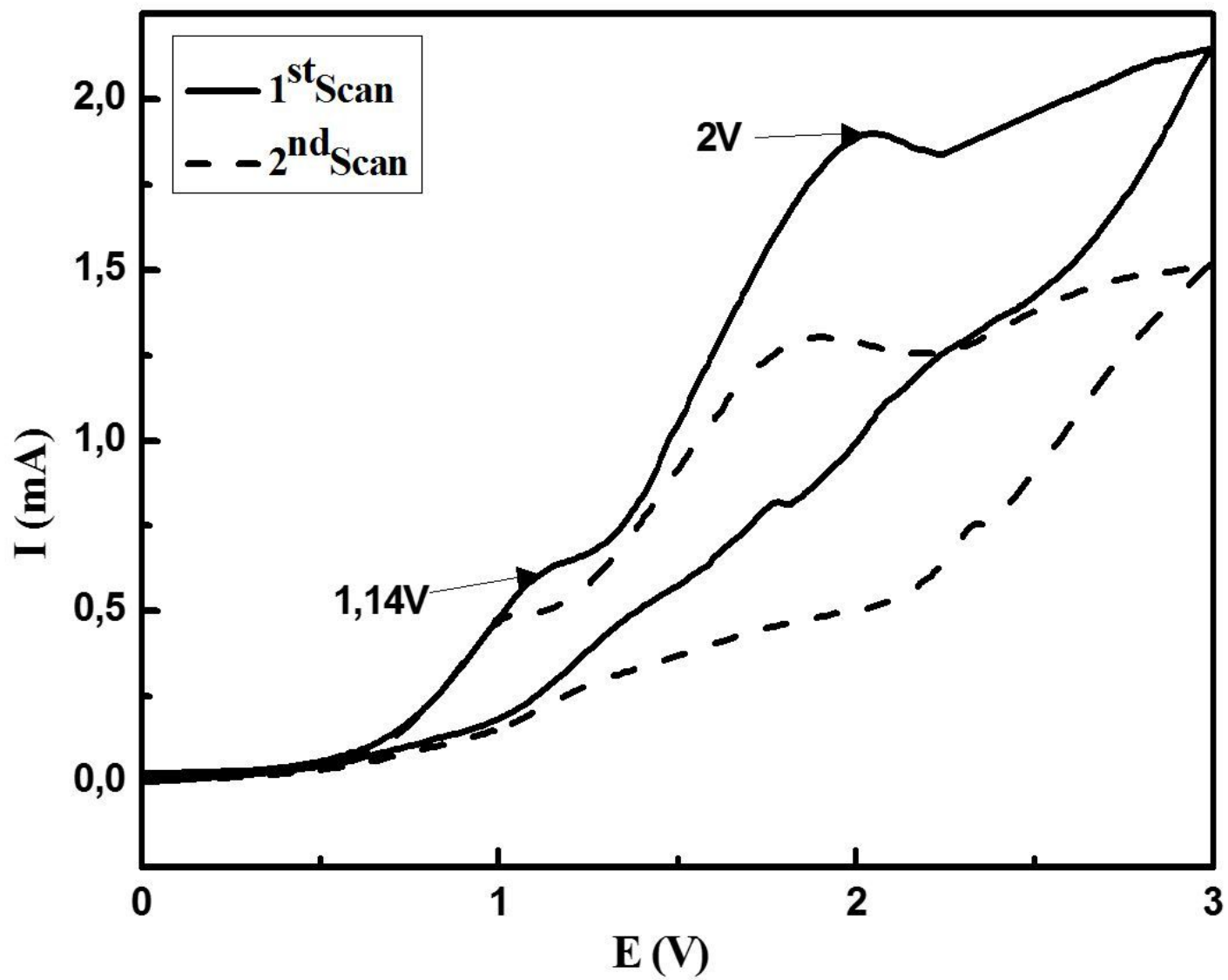
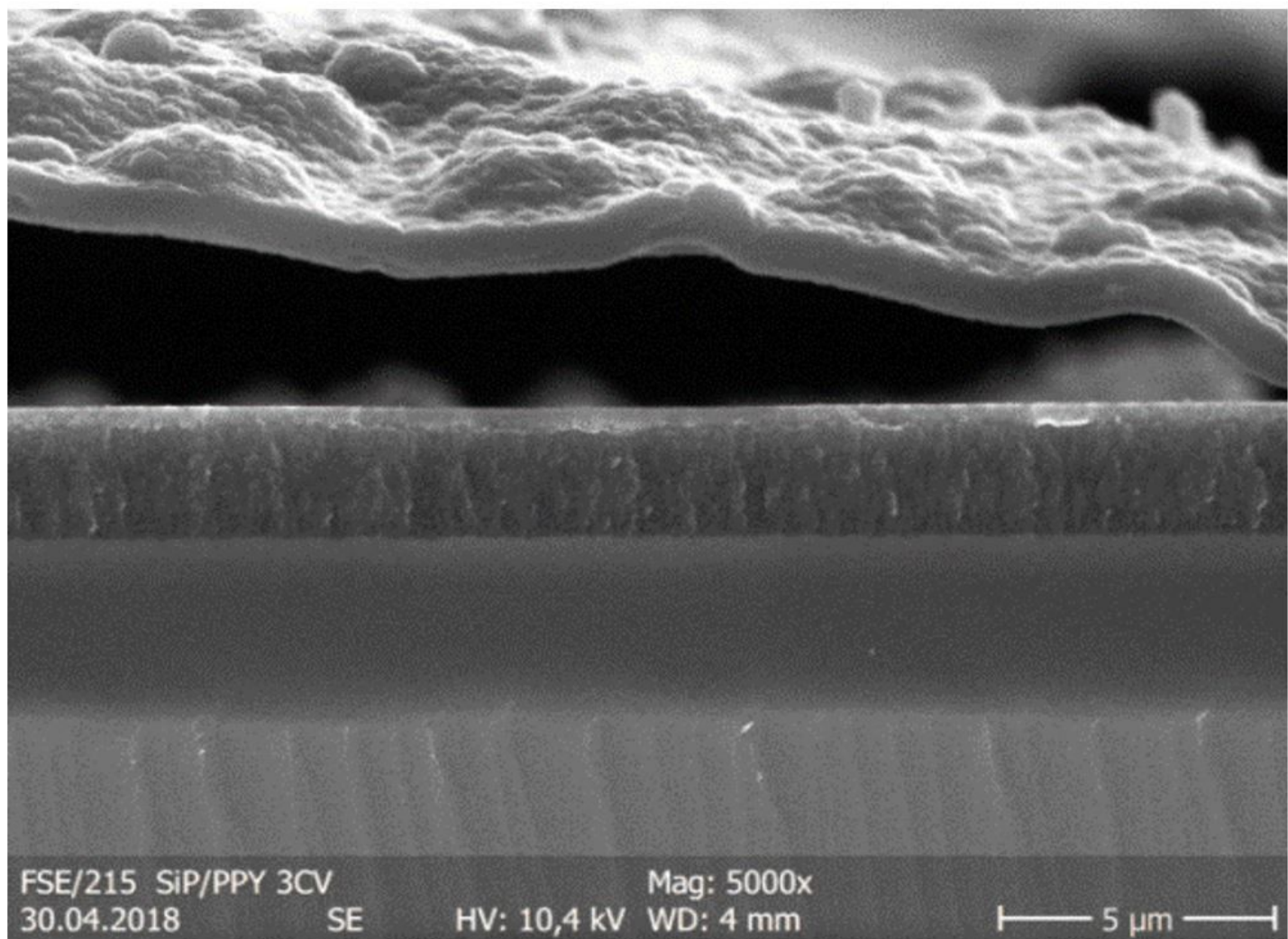


Figure 3

Cyclic voltammogram of PPy electrodeposition on mesoporous silicon at a potential sweep rate of 50 mV s<sup>-1</sup> in 0.1 M acetonitrile solution.



**Figure 4**

SEM micrographs of PPy film electrochemically deposited on porous silicon surface by cyclic voltammetry from  $-0.5$  V to  $2.5$  V at  $50$   $\text{mV s}^{-1}$  scan rate.

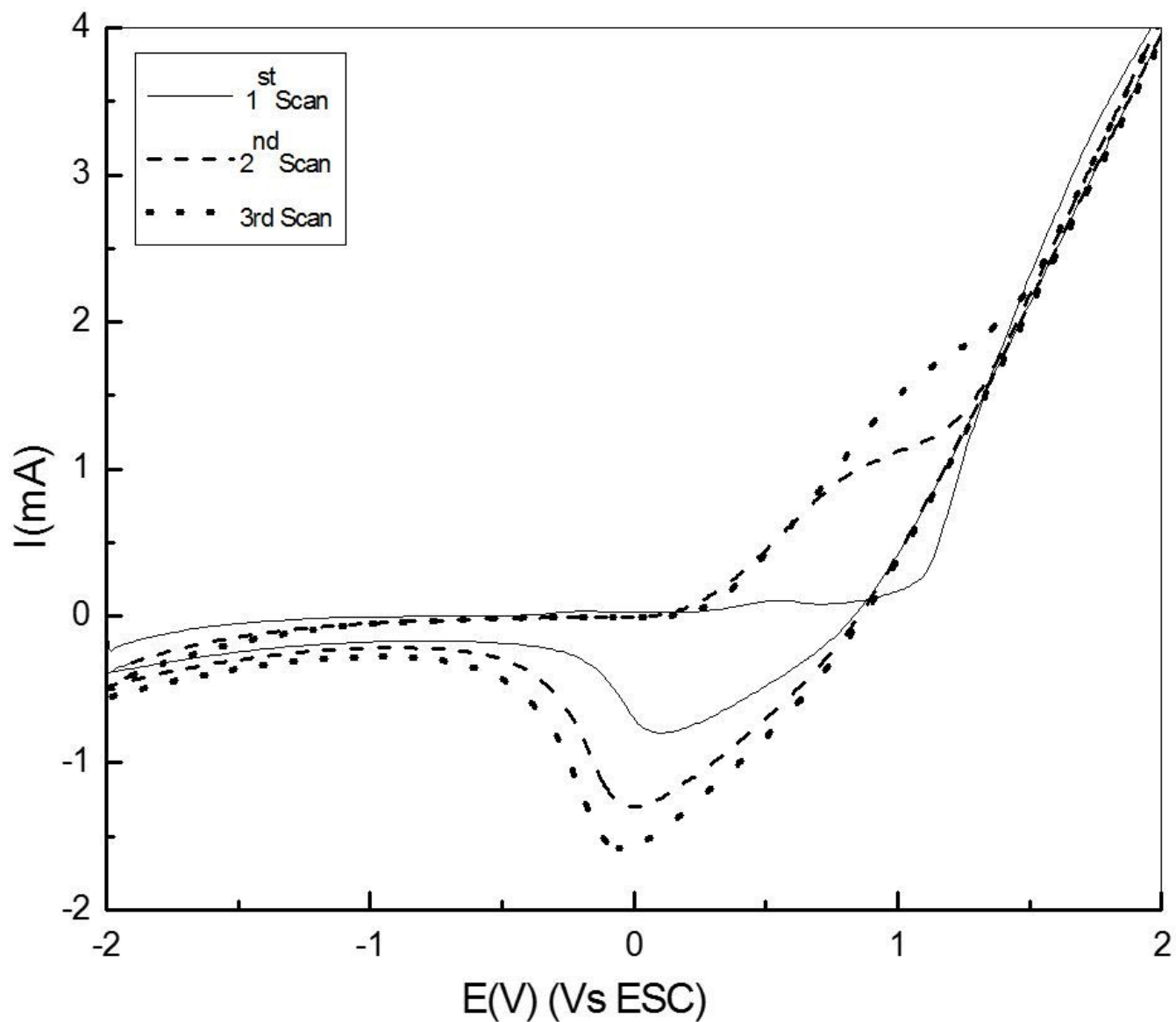


**Figure 5**

The cyclic voltammogram of PPy electrodeposition on oxidized mesoporous silicon at a potential sweep rate of  $50 \text{ mV s}^{-1}$  in  $0.1 \text{ M}$  acetonitrile solution.

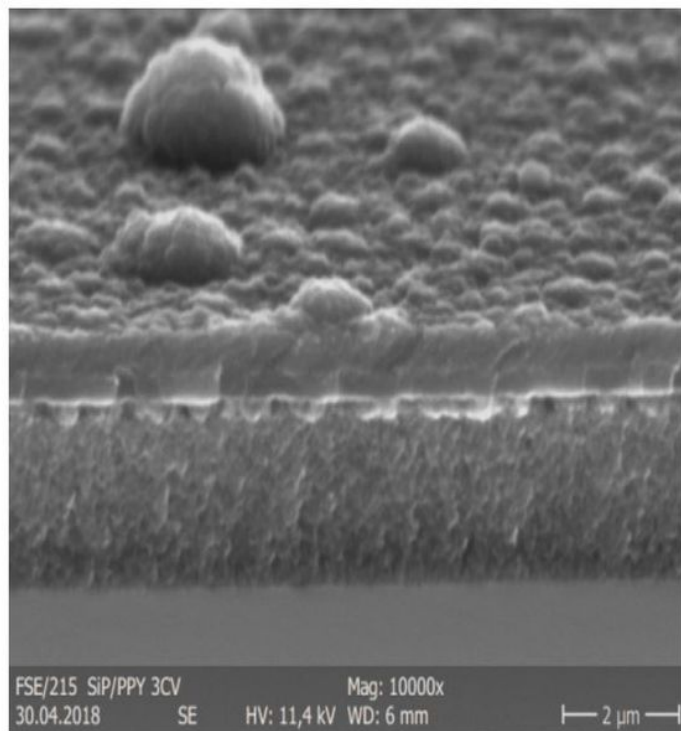
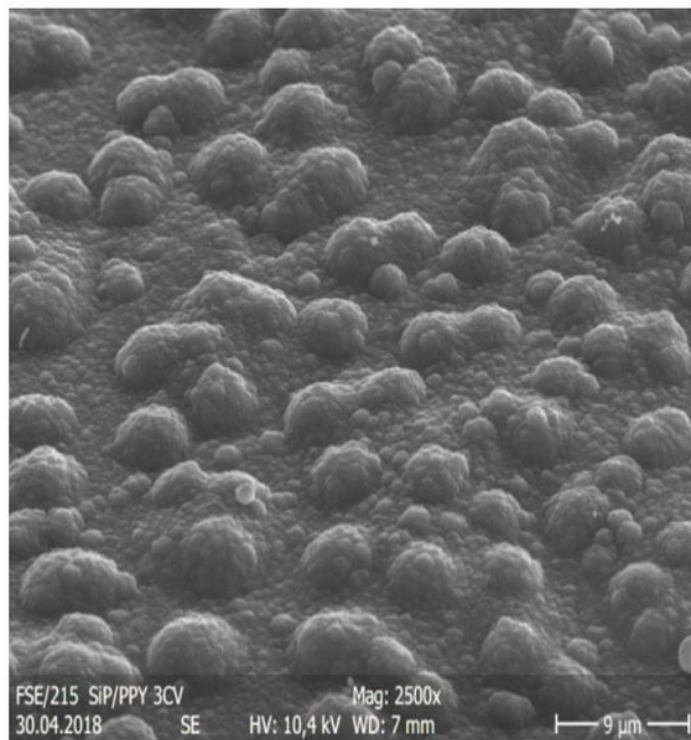


**Figure 6**

SEM micrographs of PPy film electrosynthesized on oxidized mesoporous silicon surface. a: 9 $\mu$ m and b: 2 $\mu$ m.

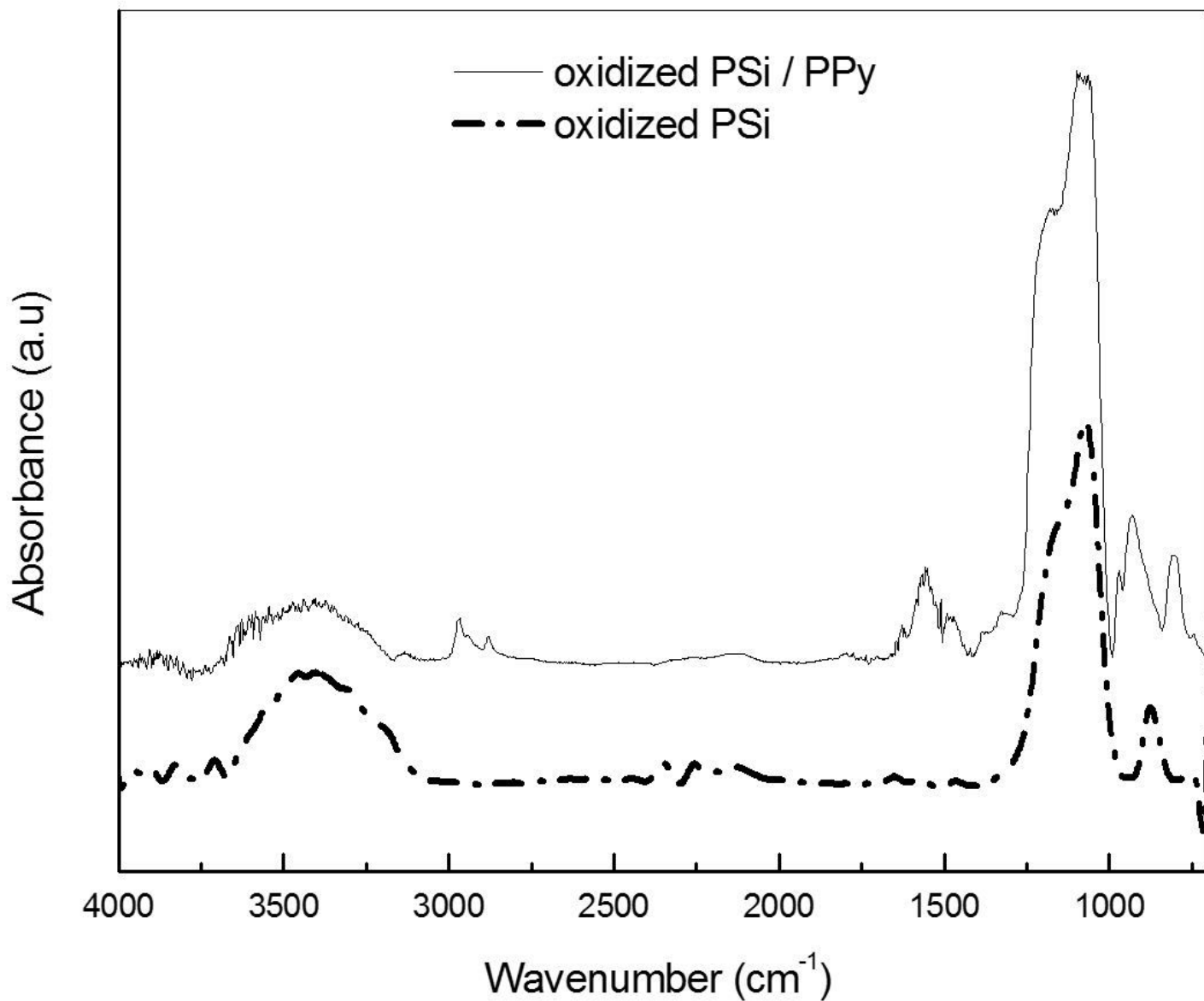
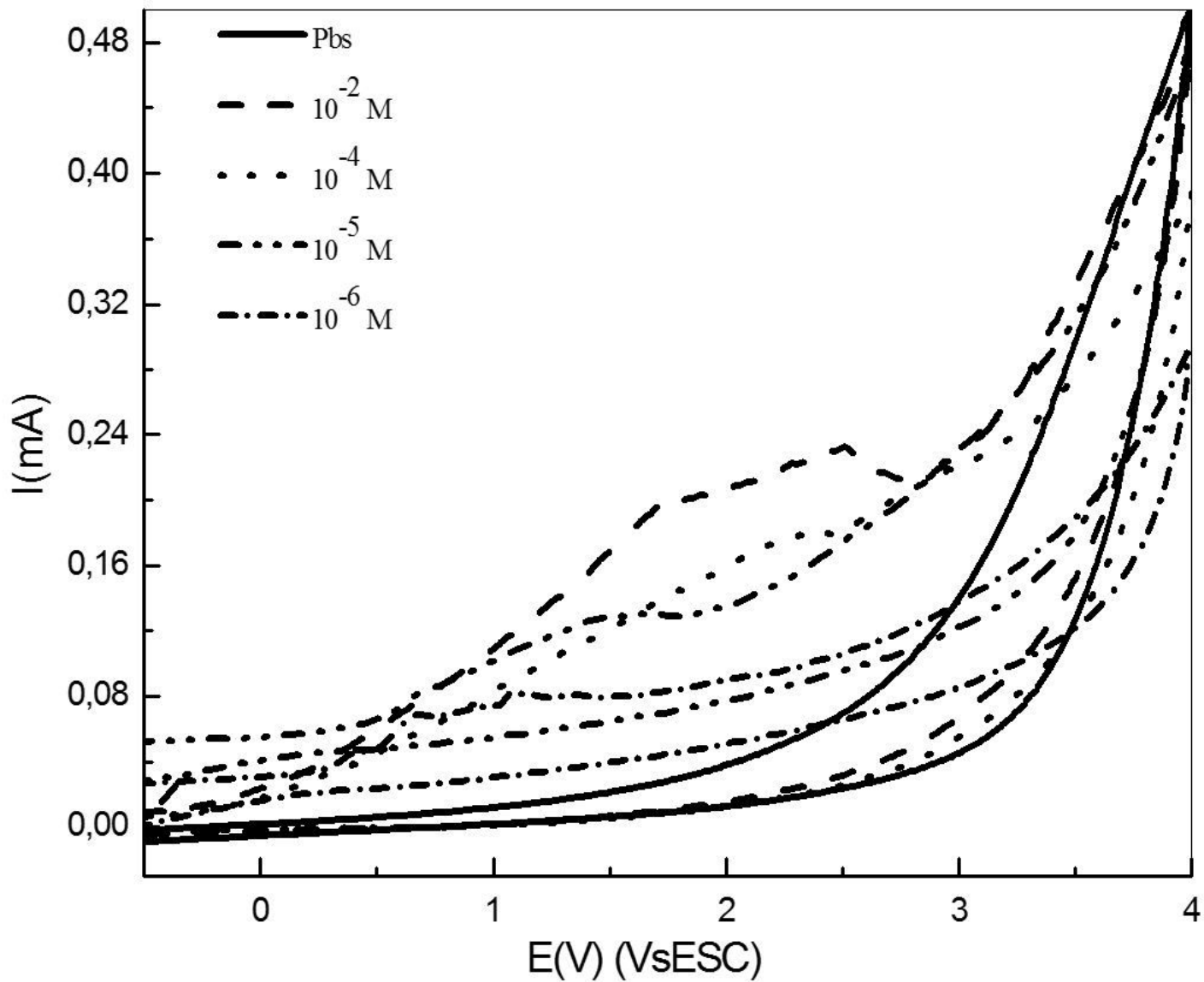


Figure 7

FTIR spectra of oxidized PSi and oxidized PSi/ PPy structure.



**Figure 8**

Voltammetric response of the hybrid structure oxidized SiP / PPy for different concentrations of para-nitrophenol ( $10^{-2}$ ,  $10^{-4}$ ,  $10^{-5}$  et  $10^{-6}$  M), in PBS (pH = 7).

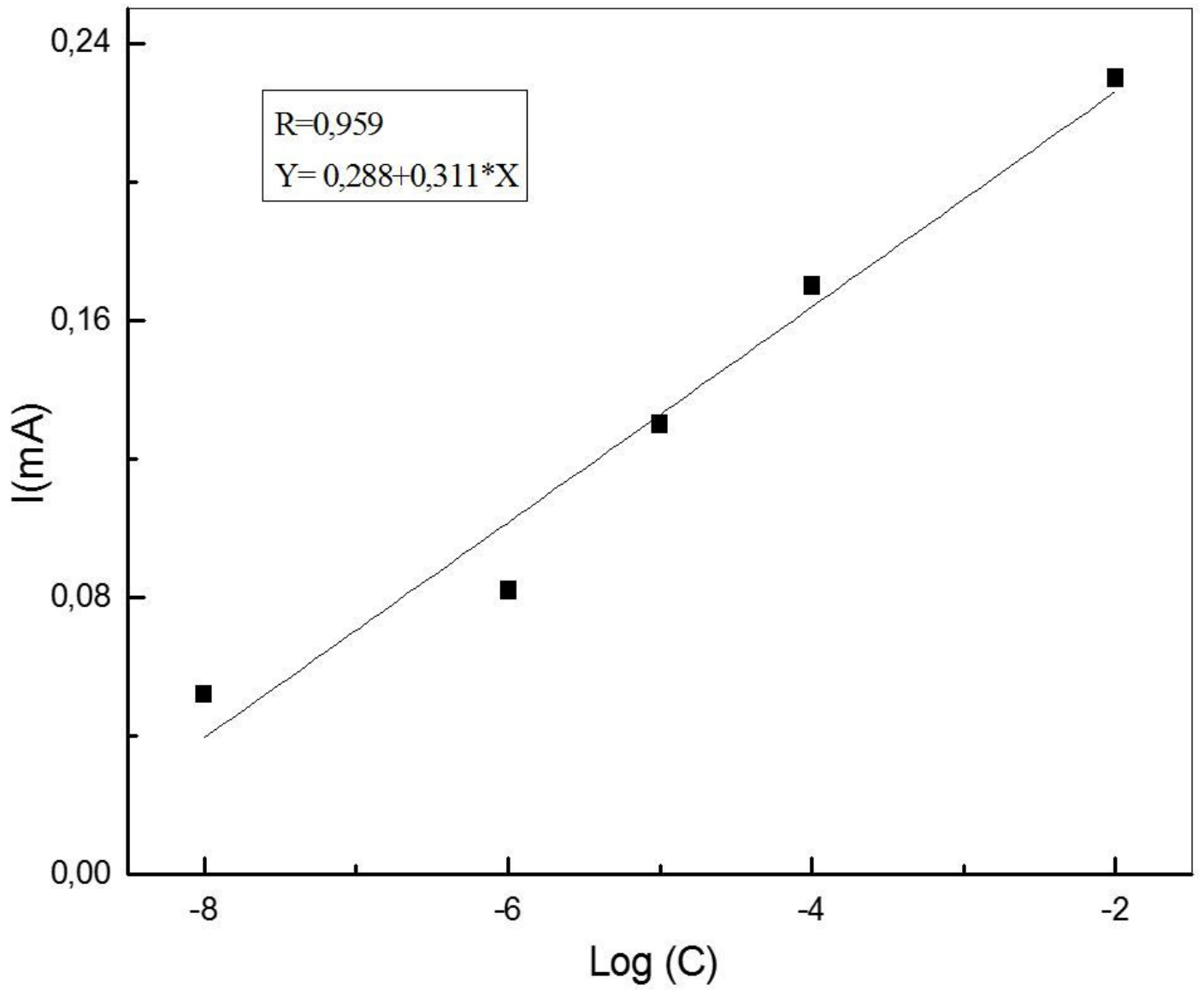


Figure 9

Calibration curve of the intensity of anodic current peaks as a function of p-Nph concentrations.